Electronic Supplementary Material (ESI) for Chemical Science.
This journal is © The Royal Society of Chemistry 2017

Supplementary Information

Reversible On-Surface Wiring of Resistive Circuits

Michael S. Inkpen,*,†,‡ Yann R. Leroux,‡ Philippe Hapiot,‡ Luis Campos,§ Latha Venkataraman*,†,§

†Department of Applied Physics and Applied Mathematics, Columbia University, New York, NY 10027, U.S.A.
‡Institut des Sciences Chimiques de Rennes (Equipe MaCSE), CNRS, UMR 6226, Université de Rennes 1, Campus de Beaulieu, Bat 10C, Rennes Cedex, France
§Department of Chemistry, Columbia University, New York, NY 10027, U.S.A.

Contents

1. Experimental details
2. Additional STM-BJ data
3. X-ray photoelectron spectra
4. Synthetic procedures
5. NMR spectra
6. References

1. Experimental details

Scanning tunneling microscope-based break junction (STM-BJ) measurements were performed using a home-built STM that has been described previously.[1] The hardware was controlled using custom software (written using IgorPro, Wavemetrics Inc., OR, USA), and experiments conducted at room temperature under ambient conditions. STM tips were prepared from freshly cut Au wire (Ø = 0.25 mm, 99.998%, Alfa Aesar), with substrates for solution experiments prepared from evaporation of >100 nm Au (≥99.95%, Alfa Aesar) at ~1 Å/s onto freshly cleaved mica or polished steel. Tip-substrate distances were controlled with sub-angstrom precision using a single-axis piezoelectric positioner (Nano-P15, Mad City Labs, WI, USA). Applying a bias between the tip and substrate, conductance was measured as a function of tip-substrate displacement (at 40 kHz acquisition rate) as the tip was repeatedly pushed into the substrate to reach a conductance of $>5\ G_0$ (where $G_0 = 2e^2/h$) and then retracted 5-10 nm (at 18 nm/s) to break the contact. The resulting conductance-distance traces were compiled into 1D conductance histograms (using logarithmic bins 100 bins/decade along the conductance axis), or 2D conductance-distance histograms (using bins of 0.002 nm along the displacement axis and 100 bins/decade along the conductance axis), without data selection. Traces in 2D histograms were aligned such that displacement = 0 nm where $G = 0.5\ G_0$. Most probable conductance values for molecules studied here were obtained through Gaussian fits to their corresponding conductance peaks in 1D histograms. Directly before starting a solution-based experiment, substrates were treated with UV/ozone for 20 min (using a NovaScan PSD UV, Novascan Technologies, Inc., IA, USA), and 1,000 traces collected to check the gold surface was free from contamination. Molecules of interest were then introduced as 0.1-1 mM solutions in 1,2,4-trichlorobenzene (TCB, Sigma-Aldrich or Alfa Aesar, 99% purity).

Unless otherwise stated, no special precautions to exclude air or moisture from *in situ* or *ex situ* reactions were taken. 8-Mercaptooctanoic acid was purified by column chromatography (SiO_2, ethyl acetate/hexanes [1:3 v/v]) before use in STM-BJ experiments, all other reagents were commercially available and used as received. ^1H and $^{13}C\{^1H\}$ NMR spectra were recorded on a Bruker DRX 300 (300 MHz), Avance III 400SL (400 MHz) or Avance III 500 (500 MHz) spectrometer and referenced to the residual solvent peaks of $CDCl_3$ at 7.26 and 77.16 ppm, respectively. Mass spectrometry analyses were conducted by Brandon Fowler of the Mass

Spectrometry Facility, Chemistry Department, Columbia University, New York using a Waters XEVO G2-XS QToF mass spectrometer.

X-ray photoelectron spectra were recorded on a PHI 5500 model spectrometer equipped with a MgKα standard (non-monochromated) X-ray source, hemispherical electron energy analyzer, and multichannel detector. Spectra were acquired using a 15 kV anode potential and 13.3 mA emission current (X-ray source power = 200 Watts), with an analyzer pass energy of 23.50 eV. The surface normal-detector take off angle was 45°, and chamber pressures during measurements were maintained at $\leq 1 \times 10^{-9}$ Torr. Binding energy scales for each sample were referenced to the Au $4f_{7/2}$ peak at 84.00 eV. Spectra of the S 2p region were obtained by averaging 5 consecutive scans to improve the signal-to-noise ratio.

2. Additional STM-BJ data

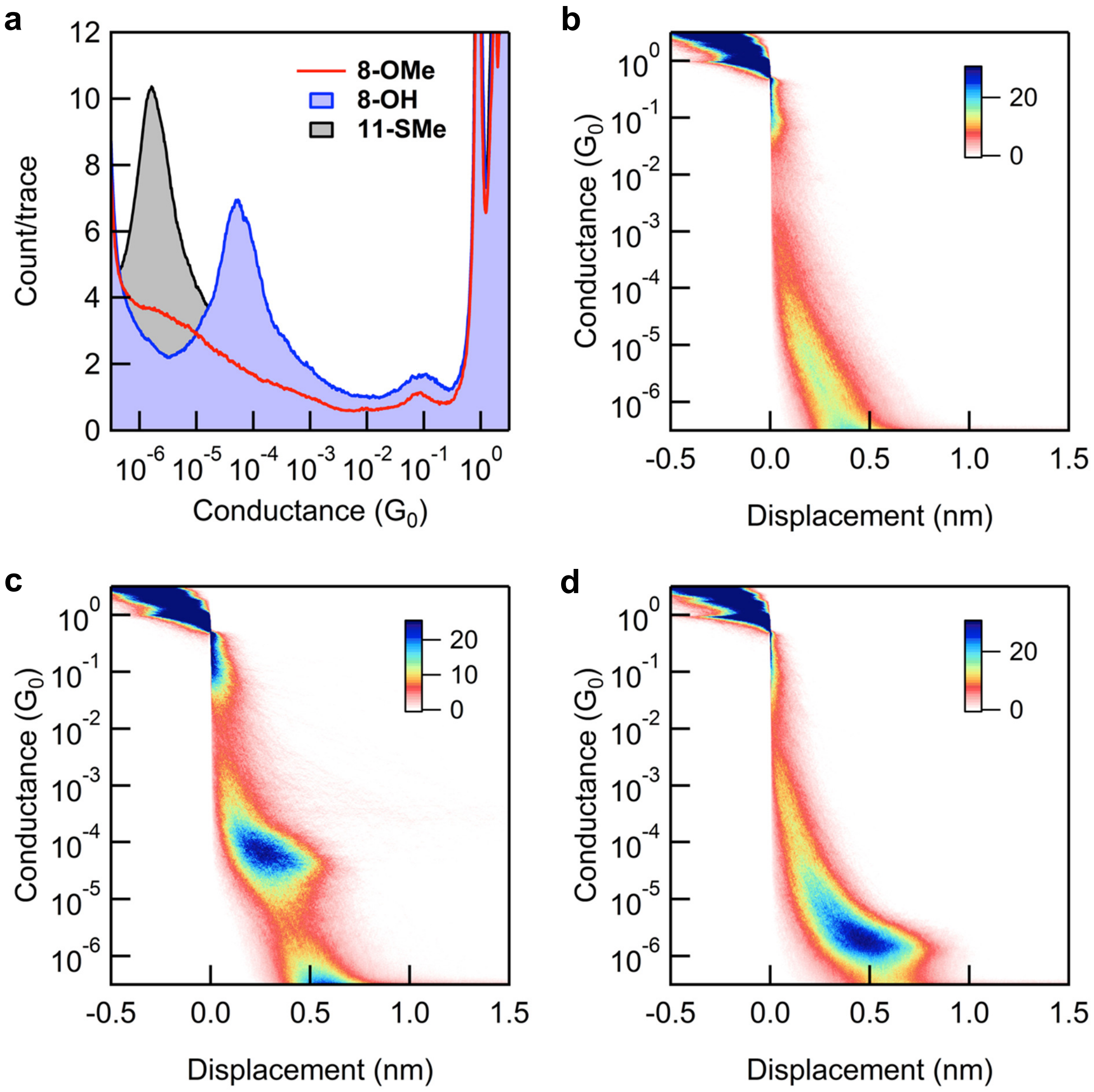

Figure S1. 1D (a) and 2D (b, c, d) conductance histograms (10,000 traces, V_{bias} = 345 mV) for **8-OMe**, **8-OH** and **11-SMe** in TCB, respectively. Color bars indicate the number of counts/1000 traces.

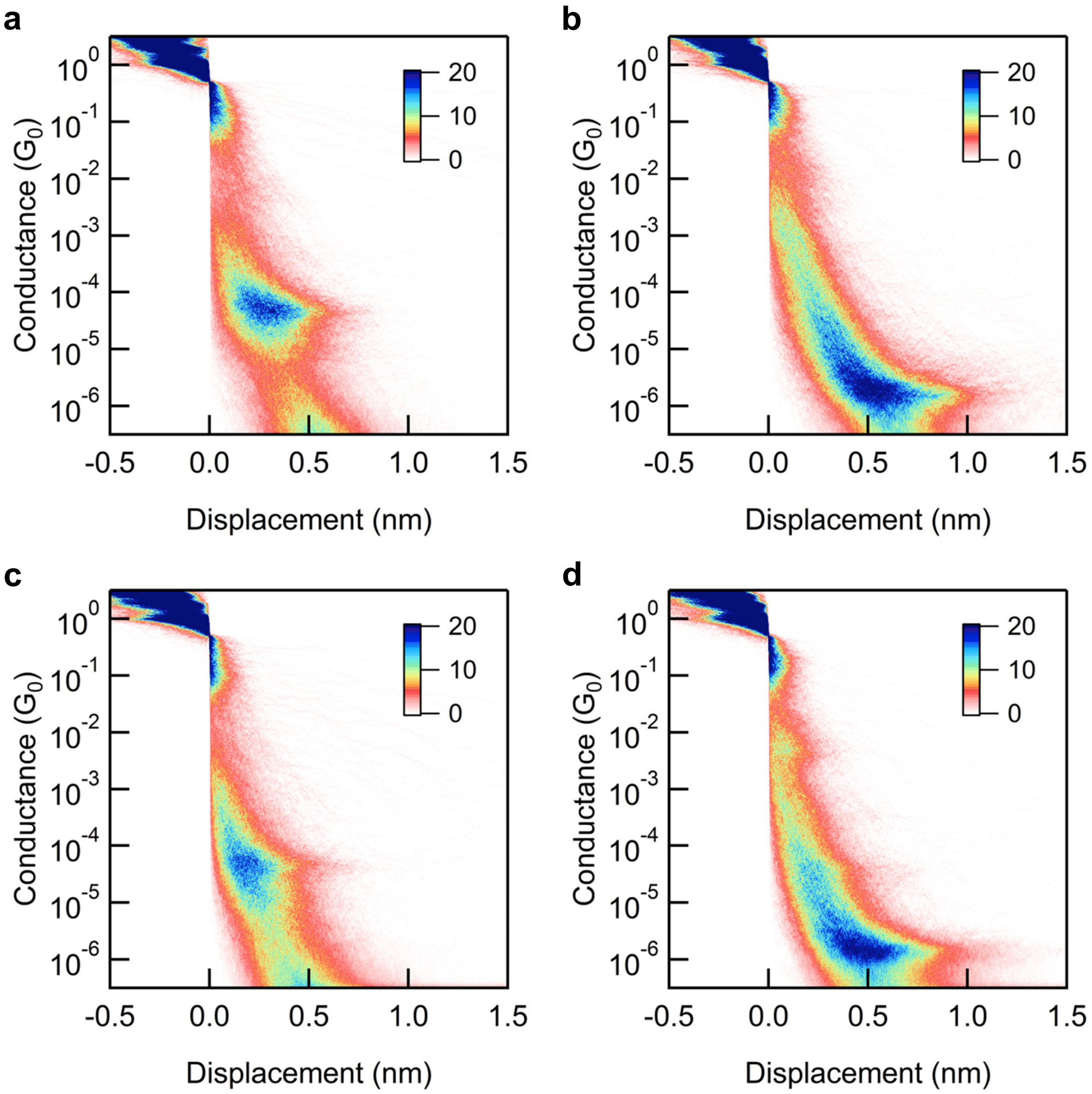

Figure S2. Representative 2D conductance histograms (5,000 traces, V_{bias} = 345 mV) for monolayers of (a) **8-OH**, (b) **11-SMe** (prepared *ex situ*), (c) **8-OH** and (d) **11-SMe** (prepared *in situ*). These correspond to the 1D histograms shown in **Figure 2b** and **Figure 3a**. Color bars indicate the number of counts/1000 traces.

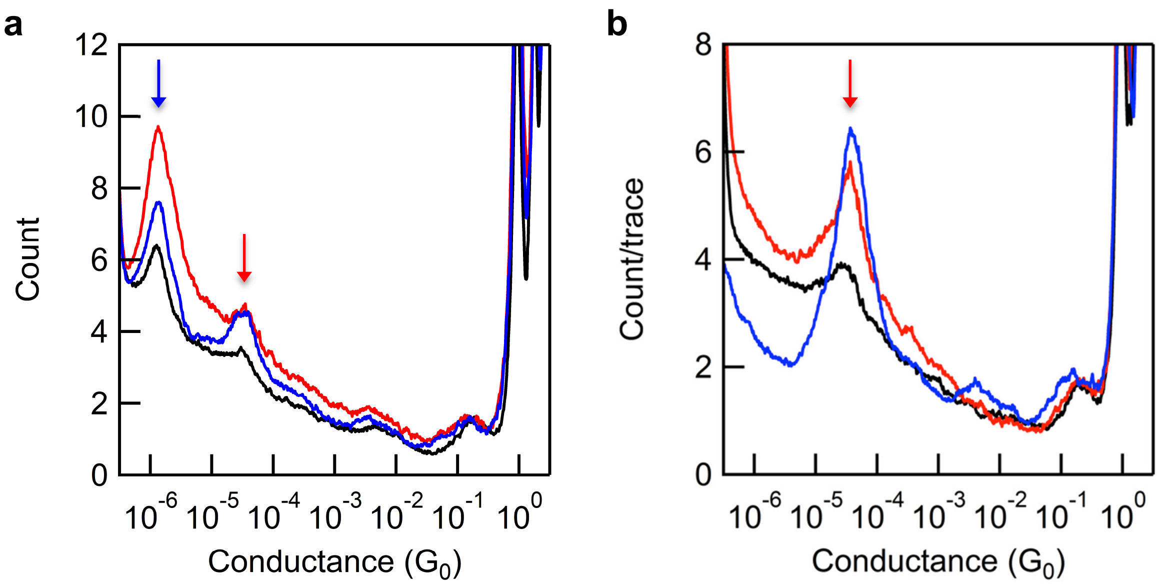

Figure S3. Additional 1D conductance histograms (5,000 traces, V_{bias} = 345 mV) obtained from measurements of undiluted **8-OH** monolayers after *in situ* Steglich esterification for 24 h at r.t. using (a) DIC or (b) DCC. The relative intensities of reactant and product peaks (indicated by red and blue arrows, respectively) represent the extent of conversion. Though yields for DIC are variable (see also the example in **Figure 3a**), they are always superior to DCC. Each histogram was obtained from measurements made on a different substrate.

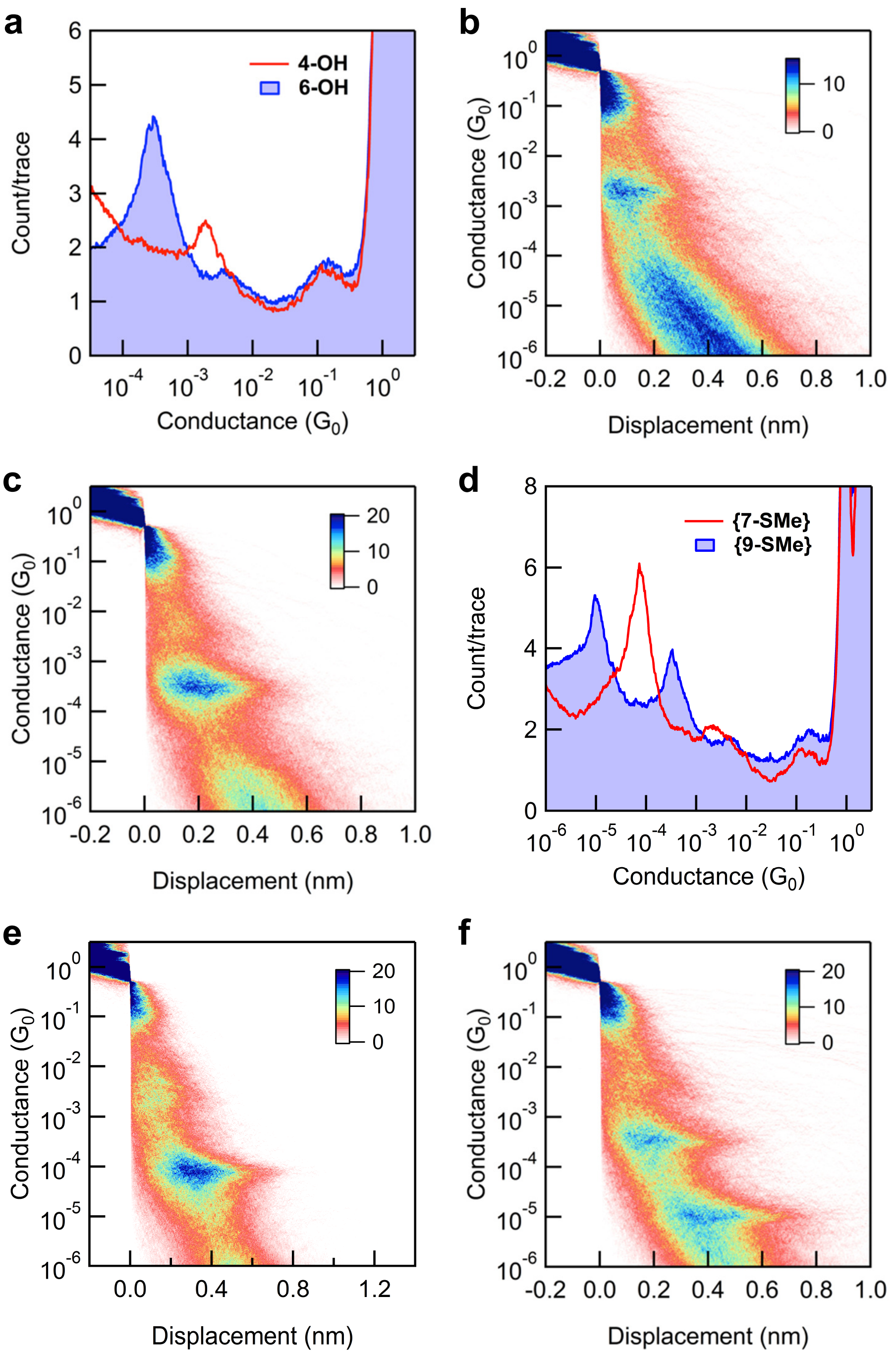

Figure S4. Representative 1D (a) and 2D (b, c) conductance histograms generated from 5,000 traces for **4-OH** and **6-OH** monolayers (V_{bias} = 345 mV), respectively. 1D (d) and 2D (e, f) conductance histograms generated from 5,000 traces for *in situ* synthesized **7-SMe** and **9-SMe**, respectively (V_{bias} = 345 mV). Color bars indicate the number of counts/1000 traces.

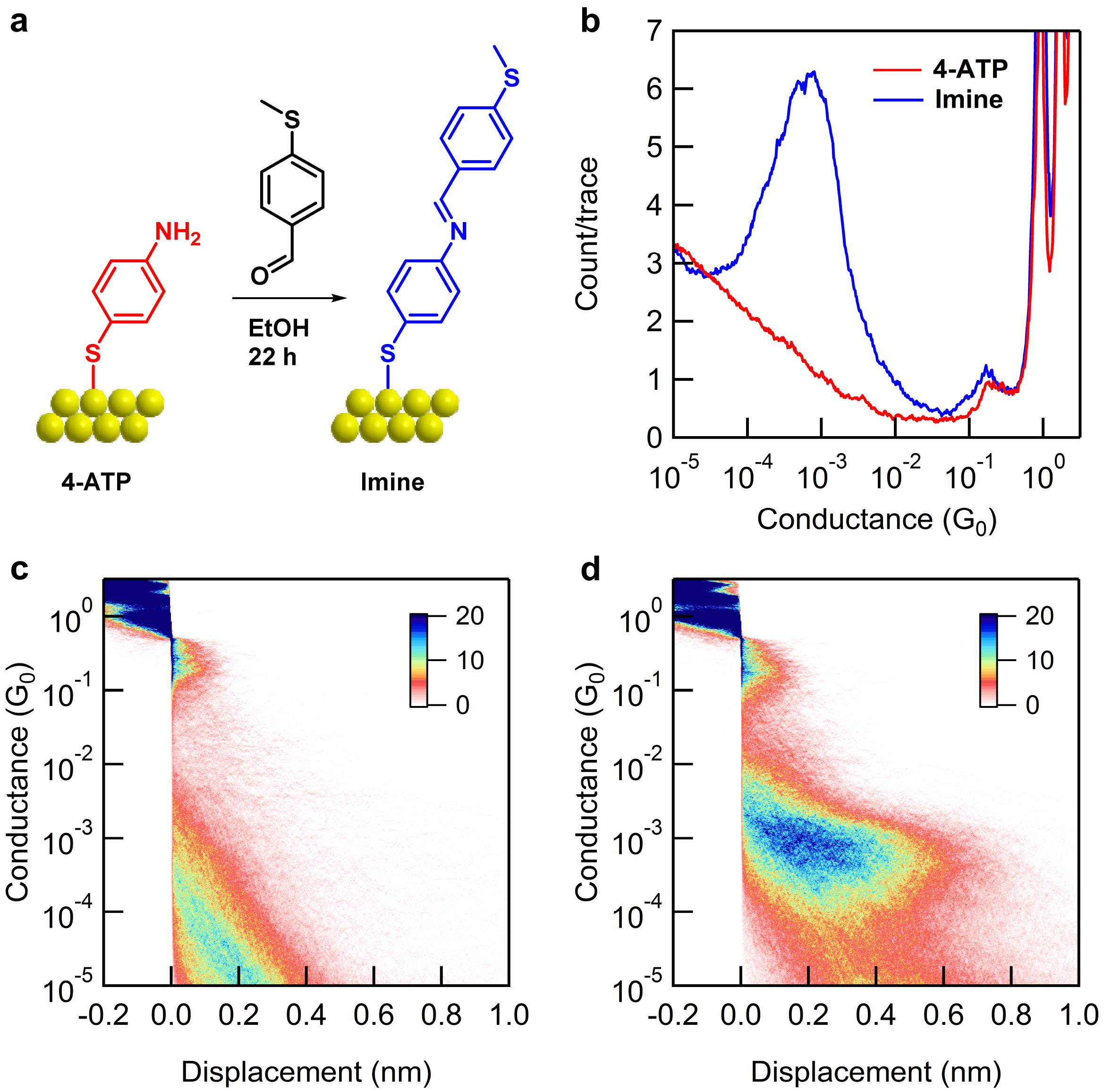

Figure S5. (a) Molecular structures and reaction conditions for the surface-based imine dehydration reaction. Representative 1D (b) and 2D (c, d) conductance histograms generated from 5,000 traces for 4-aminothiophenol (**4-ATP**) and *in situ* synthesized imine product monolayers (V_{bias} = 230 mV), respectively. Color bars indicate the number of counts/1000 traces.

3. X-ray photoelectron spectra

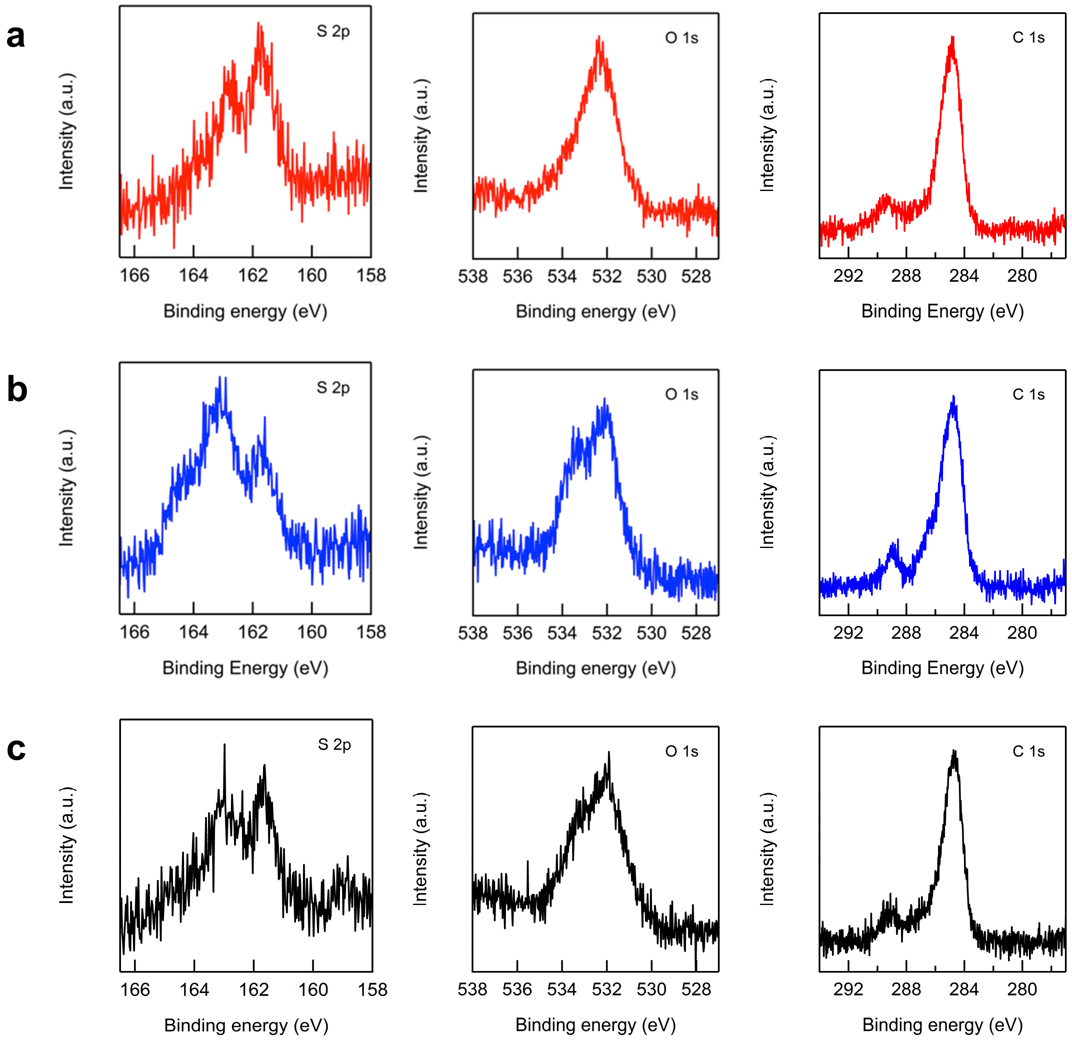

Figure S6. X-ray photoelectron spectra (S 2p, O 1s and C 1s regions) for SAMs of: (a) **8-OH** (one S and O environments); (b) **11-SMe** (two S and O environments); (c) **11-SMe** prepared by *in situ* esterification from a SAM of **8-OH**. The data in (c) indicates the monolayer of **8-OH** is not displaced during the surface-based reaction. Furthermore, the success of the latter is corroborated by the increased O 1s peak width in (c), consistent with the broadened O 1s peak (two environments) observed for the *ex situ* synthesized product monolayer in (b). In stark contrast, STM-BJ measurements (e.g. **Figure S3**) provide much clearer (even potentially quantitative) information relating to the success of such *in situ* reactions. We note that in (b) and (c), the somewhat limited attenuation of the 162 eV doublet in S 2p spectra (assigned to Au-bound S) is consistent with some fraction of the monolayer being disordered or lying down.

4. Synthetic procedures

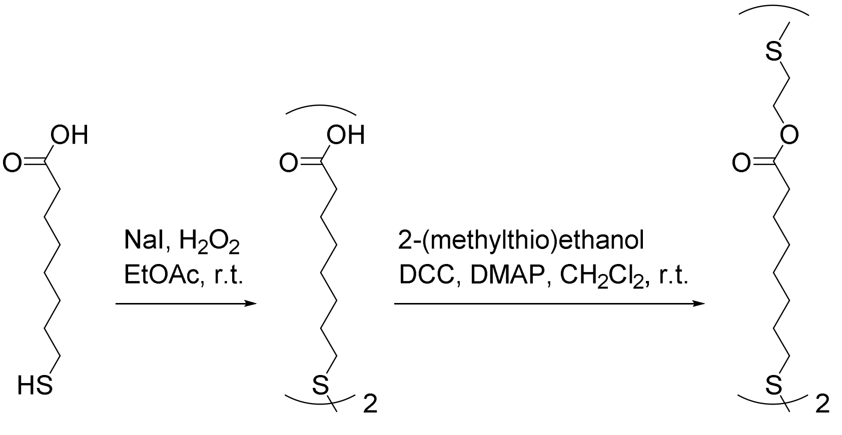

8-OH **1** **11-SMe**

Scheme S1. Synthetic route to **11-SMe**.

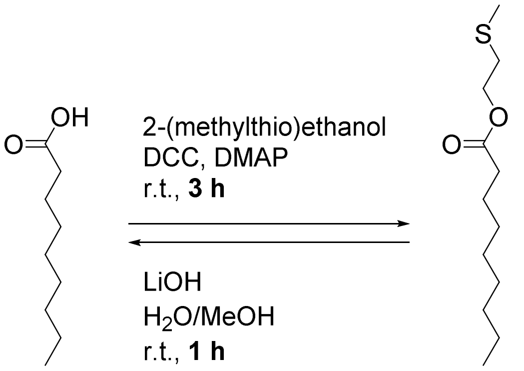

2 (68%) **3** (94%)

Scheme S2. Esterification and hydrolysis reactions with a model system. High isolated yields after short reaction times confirm these conditions are effective *ex situ*.

*Methyl 8-mercaptooctanoate (**8-OMe**)*

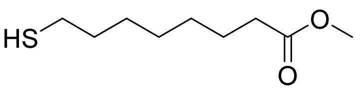

This synthetic route was adapted from an analogous procedure.[2] A solution of 8-mercaptooctanoic acid (0.099 g, 0.562 mmol) in methanol (5 mL) was acidified with conc. H_2SO_4 (2 drops) and sparged with argon (5 min). After stirring at 55 °C (water bath) under argon for 3 h, the mixture was cooled to room temperature, diluted with H_2O (10 mL) and extracted with CH_2Cl_2 (3 x 20 mL). The organic extracts were combined and volatile components removed under vacuum, whereby the residue was extracted into hexanes and purified using a SiO_2 column packed with hexanes, eluting with CH_2Cl_2-/hexanes (1:1 v/v, TLC plates visualized with iodine). Selected fractions were combined to yield a pale yellow low melting point solid/oil (0.089 g, 83%). ^1H NMR (300 MHz, $CDCl_3$): δ (ppm) 1.31 (m, 5H, -CH_2- and -SH), 1.38 (m, 2H, -CH_2-), 1.61 (m, 4H, -CH_2-), 2.30 (t, 2H, J = 7.5 Hz, -CH_2C(O)-), 2.51 (dt, 2H, J = 4.8, 8.6 Hz, -CH_2SH), 3.67 (s, 3H, -OCH_3). $^{13}C\{^1H\}$ NMR (75 MHz, $CDCl_3$): δ (ppm) 24.72, 25.00, 28.29, 28.83, 29.13, 34.07, 34.18, 51.58 (-COO*C*H_3), 174.34 (-*C*OOCH_3). HRMS (ASAP–): m/z 189.0951 ($[M-H]^-$ calc. for $C_9H_{17}O_2S$: 189.0949).

*8,8′-Disulfanediyldioctanoic acid (**1**)*

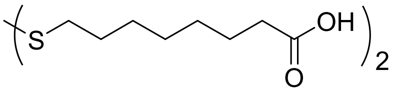

This synthetic route was adapted from an analogous procedure.[3] Hydrogen peroxide (50 wt. % in H_2O, 0.16 mL, 2.8 mmol) was added with stirring to 8-mercaptooctanoic acid (0.413 g, 2.34 mmol) and sodium iodide (0.006 g, 0.04 mmol) in ethyl acetate (6.8 mL). After stirring for 1.5 h at 20°C, the yellow-brown mixture was poured into saturated *aq.* $Na_2S_2O_3$ (30 mL). The aqueous layer was extracted with ethyl acetate (3 x 20 mL), and the combined organic phase dried over Na_2SO_4, filtered and solvent removed *in vacuo*. The crude material was purified via chromatography using a SiO_2 column packed with MeOH:CH_2Cl_2 (1:99 v/v), eluting with MeOH:CH_2Cl_2 (5:95 →1:9 v/v). The product was obtained as a white solid (0.060 g, 15%). ^1H NMR (500 MHz, $CDCl_3$): δ (ppm) 1.37 (m, 12H, -CH_2-), 1.66 (m, 8H, -CH_2-), 2.36 (t, 4H, J = 7.2 Hz, -CH_2-), 2.68 (t, 4H, J = 7.3 Hz, -CH_2-), 11.19 (br s, 2H, -COOH). $^{13}C\{^1H\}$ NMR (126 MHz, $CDCl_3$): δ (ppm) 24.69, 28.31, 28.80, 28.85, 29.12, 34.07, 39.35, 179.86 (-*C*OOH). HRMS (ASAP–): m/z 349.1509 ($[M-H]^-$ calc. for $C_{16}H_{29}O_4S_2$: 349.1507).

*Bis(2-(methylthio)ethyl) 8,8′-disulfanediyldioctanoate (**11-SMe**)*

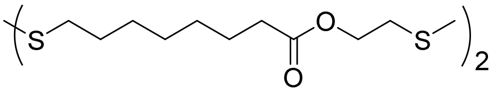

A stirred solution of **1** (0.044 g, 0.13 mmol), 4-dimethylaminopyridine (0.007 g, 0.06 mmol) and 2-(methylthio)ethanol (0.26 mL, 3.0 mmol) in CH_2Cl_2 (0.5 mL) was cooled to 5°C (ice bath), whereby N,N'-dicyclohexylcarbodiimide (0.223 g, 1.08 mmol) was added, as well as additional CH_2Cl_2 (0.5 mL) to rinse the walls of the flask. After 5 min the reaction mixture was raised to room temperature and stirred for a further 3 h, whereby the resulting slurry was filtered and solvent removed under vacuum. The residue was loaded in hexanes onto a SiO_2 column packed with hexanes, eluting with hexanes/CH_2Cl_2/MeOH (1:1:0→0:1:0→0:95:5 v/v, TLC plates visualized with basic $KMnO_4$). Combination of desired fractions and solvent removal provided the product as a pale yellow oil (0.013 g, 21%). ^{1}H NMR (500 MHz, $CDCl_3$): δ (ppm) 1.33 (m, 8H, -CH_2-), 1.39 (m, 4H, -CH_2-), 1.65 (m, 8H, -CH_2-), 2.16 (s, 6H, -SCH_3), 2.32 (t, 4H, J = 7.5 Hz, -CH_2-), 2.67 (t, 4H, J = 7.4 Hz, -CH_2-), 2.72 (t, 4H, J = 6.8 Hz, -CH_2-), 4.25 (t, 4H, J = 6.8 Hz, -CH_2-). ^{13}C{^{1}H} NMR (126 MHz, $CDCl_3$): δ (ppm) 15.95, 24.98, 28.47, 29.02, 29.13, 29.28, 32.79, 34.33, 39.21, 62.97 (-C[=O]OCH$_2$-), 173.71 (-C[=O]O-). HRMS (ESI+): m/z 521.1865 ($[M+Na]^+$ calc. for $C_{22}H_{42}O_4S_4Na$: 521.1864).

*Octanoic acid (**2**)*

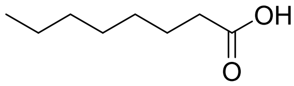

<u>From methyl octanoate:</u> This synthetic route was adapted from an analogous procedure.[4] A solution of sodium hydroxide (2.90 g, 72.5 mmol) in methanol (32 mL) was added to methyl octanoate (5.7 mL, 32 mmol) in CH_2Cl_2 (285 mL). After stirring for 2 h at room temperature, volatile components were removed under vacuum. The residue was dissolved in water (200 mL), and the solution extracted with diethyl ether (3 x 100 mL). The aqueous layer was cooled (ice bath) and carefully acidified to pH 2-3 (addition of 1M HCl in ~1 mL portions), whereby it was extracted with CH_2Cl_2 (3 x 100 mL). The combined organic extracts were dried over Na_2SO_4, before filtration and removal of solvent under vacuum to provide a pale yellow low melting point solid/oil (4.321 g, 95%). ^{1}H NMR (500 MHz, $CDCl_3$): δ (ppm) 0.88 (t, 3H, J = 7.0 Hz, -CH_3), 1.30 (m, 8H, -CH_2-), 1.64 (quint., 2H, J = 7.4 Hz, -CH_2-), 2.35 (t, 2H, J = 7.5 Hz, -CH_2COOH), 10.73 (br s, 1H, -COOH). ^{13}C{^{1}H} NMR (101 MHz, $CDCl_3$): δ (ppm) 14.20, 22.74, 24.84, 29.05, 29.17, 31.78, 34.16, 180.02 (-COOH). HRMS (ASAP–): m/z 143.1073 ($[M-H]^-$ calc. for $C_8H_{15}O_2$: 143.1072).

<u>From **3** (*in situ* hydrolysis conditions):</u> A solution of LiOH (0.27 g, 11 mmol) in H_2O/MeOH (20 mL, 7:2 v/v) was added to **3** (0.5 g, 2.3 mmol), and the mixture was stirred for 1 h at room temperature. The aqueous layer was acidified to pH 2 by careful addition of 10% HCl w/v, and then extracted with diethyl ether (3 x 50 mL). The combined organic extracts were dried over $MgSO_4$, filtered, and solvent removed *in vacuo*. The crude product was purified by chromatography using first a SiO_2 column packed with hexanes, eluting with hexanes/ethyl

acetate (85:15 v/v/), then a SiO_2 column packed with CH_2Cl_2, eluting with CH_2Cl_2/MeOH (1:0→95:5 v/v, TLC plates visualized with basic $KMnO_4$). Selected fractions were combined in each case and solvent removed to provide a yellow oil (0.224 g, 68%). ^{1}H NMR spectroscopic features were identical to those of the product obtained from methyl octanoate.

*2-(Methylthio)ethyl octanoate (**3**)*

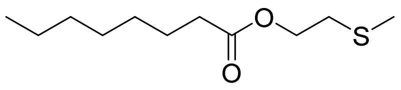

CH_2Cl_2 as solvent: A stirred solution of octanoic acid (1.85 g, 12.8 mmol), 4-dimethylaminopyridine (0.006 g, 0.051 mmol) and 2-(methylthio)ethanol (3.6 mL, 41.4 mmol) in CH_2Cl_2 (10 mL) was cooled to 5°C (ice bath), whereby N,N'-dicyclohexylcarbodiimide (3.590 g, 17.39 mmol) was added, as well as additional CH_2Cl_2 (4 mL) to rinse the walls of the flask. After 5 min the reaction mixture was raised to room temperature and stirred for a further 3 h, whereby the resulting slurry was filtered and solvent removed under vacuum. The residue was loaded in hexanes onto a SiO_2 column packed with hexanes, eluting with CH_2Cl_2/hexanes (1:1 v/v, TLC plates visualized with basic $KMnO_4$). Combination of desired fractions and solvent removal provided the product as a colorless oil (2.551 g, 91%). ^{1}H NMR (400 MHz, $CDCl_3$): δ (ppm) 0.88 (t, 3H, J = 6.9 Hz, -CH_2-), 1.29 (m, 8H, -CH_2-), 1.63 (quint., 2H, J = 7.4 Hz, -CH_2-), 2.16 (s, 3H, -SCH_3), 2.32 (t, 2H, J = 7.5 Hz, -CH_2-), 2.72 (t, 2H, J = 6.8 Hz, -CH_2-), 4.25 (t, 2H, J = 6.8 Hz, -CH_2-). $^{13}C\{^1H\}$ NMR (101 MHz, $CDCl_3$): δ (ppm) 14.21, 15.95, 22.74, 25.09, 29.06, 29.24, 31.81, 32.79, 34.41, 62.98 (-C[=O]O*C*H_2-), 173.82 (-*C*[=O]O-). 2-(Methylthio)ethanol as solvent (*in situ* esterification conditions): Following the above method, using 2-(methylthio)ethanol (2 mL, 22.51 mmol), octanoic acid (0.226 g, 1.57 mmol), 4-dimethylaminopyridine (0.007 g, 0.06 mmol) and N,N'-dicyclohexylcarbodiimide (0.375 g, 1.81 mmol) yielded **3** (0.322 g, 94%). Diethyl ether as solvent: Following the above method, using diethyl ether (7 mL), 2-(methylthio)ethanol (1.8 mL, 20.26 mmol), octanoic acid (1.00 g, 6.93 mmol), 4-dimethylaminopyridine (0.034 g, 0.28 mmol) and N,N'-dicyclohexylcarbodiimide (1.612 g, 7.814 mmol) yielded **3** (1.384 g, 91%). Spectroscopic features of **3** were identical in every case.

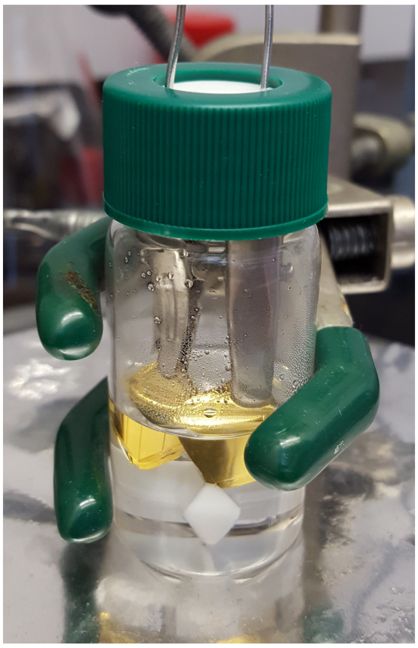

Figure S7. Typical experimental setup for *in situ* esterification reactions.

5. NMR spectra

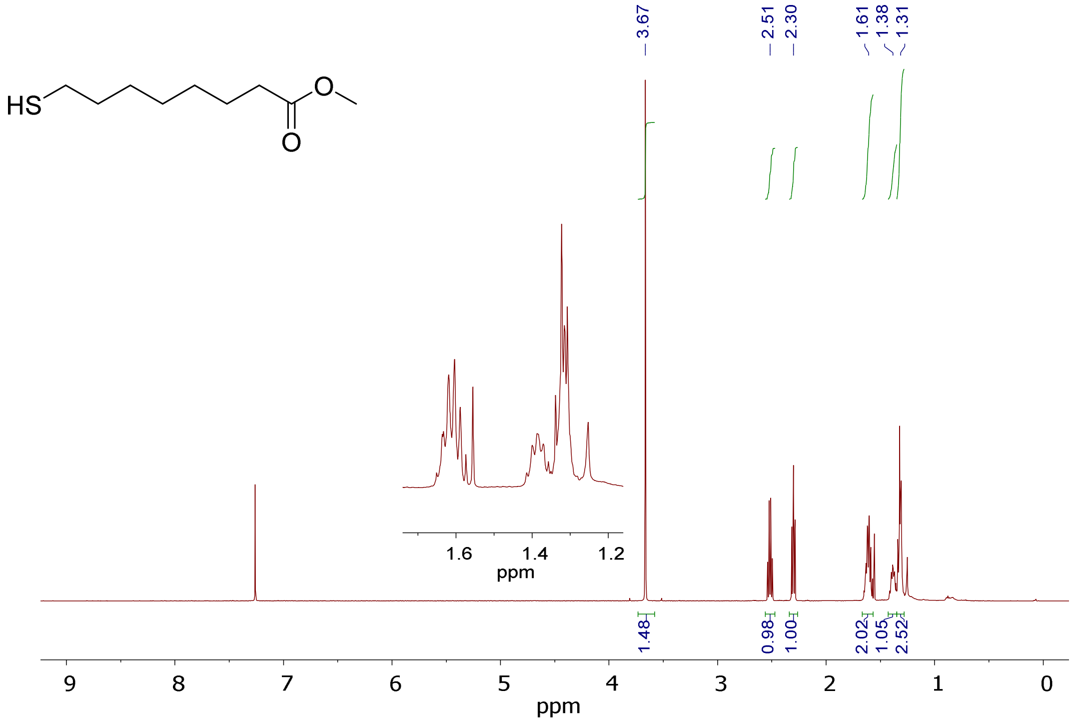

Figure S8. ^{1}H NMR spectrum of **8-OMe** in $CDCl_3$.

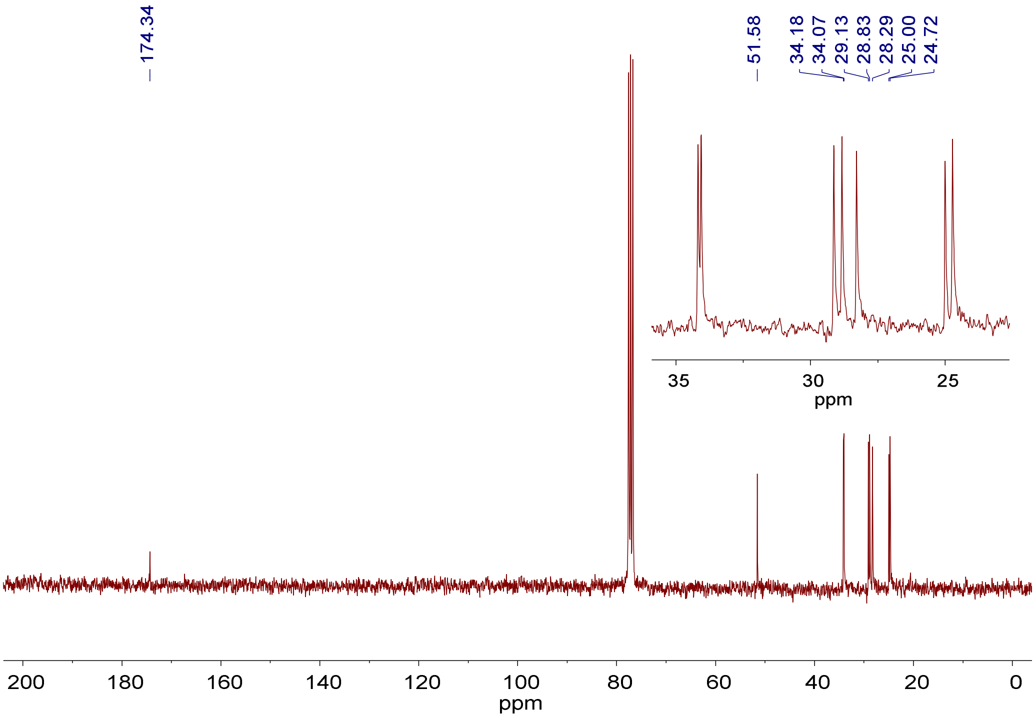

Figure S9. $^{13}C\{^{1}H\}$ NMR spectrum of **8-OMe** in $CDCl_3$.

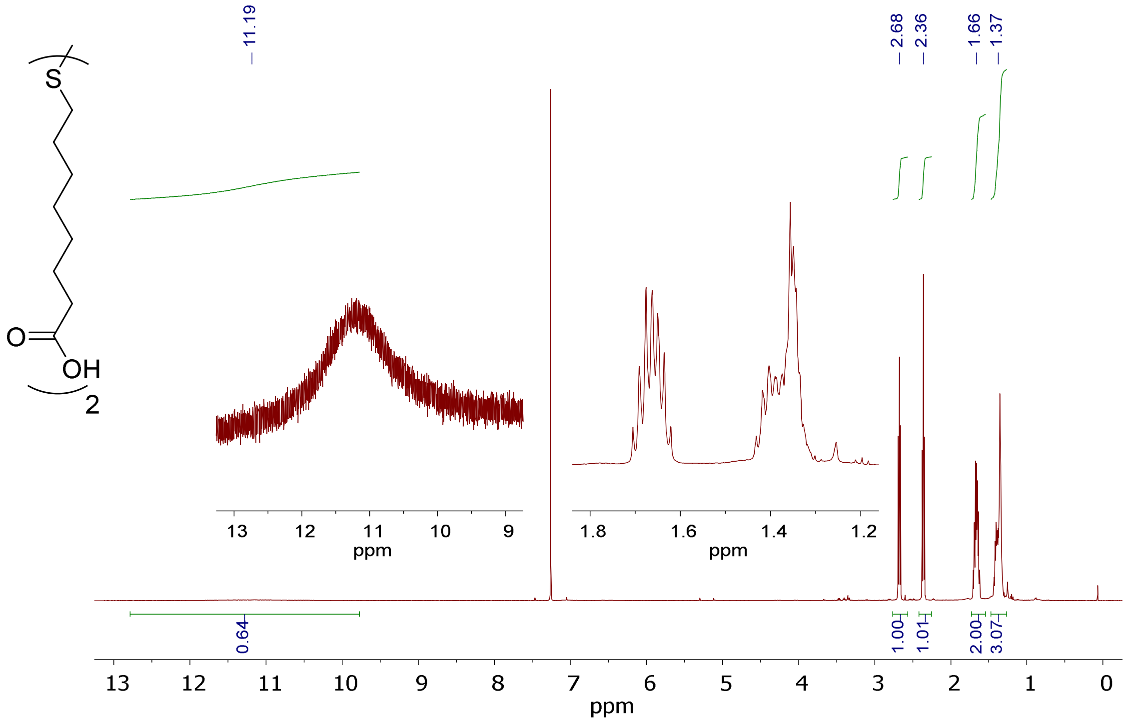

Figure S10. ^{1}H NMR spectrum of **1** in $CDCl_3$.

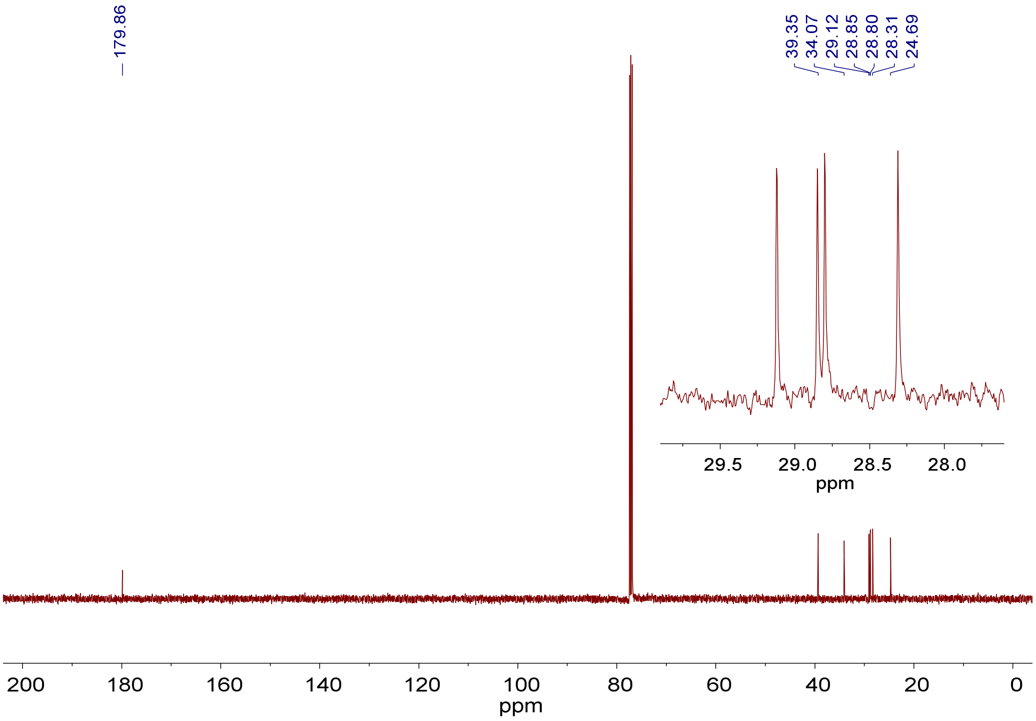

Figure S11. $^{13}C\{^{1}H\}$ NMR spectrum of **1** in $CDCl_3$.

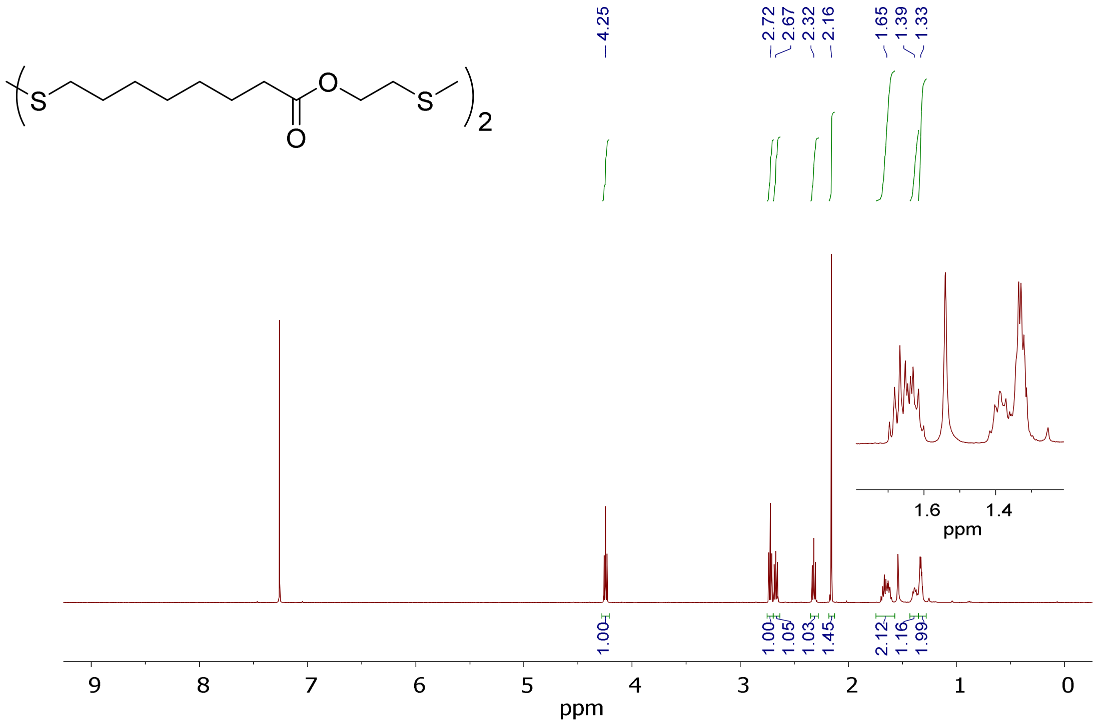

Figure S12. ^{1}H NMR spectrum of **11-SMe** in $CDCl_3$.

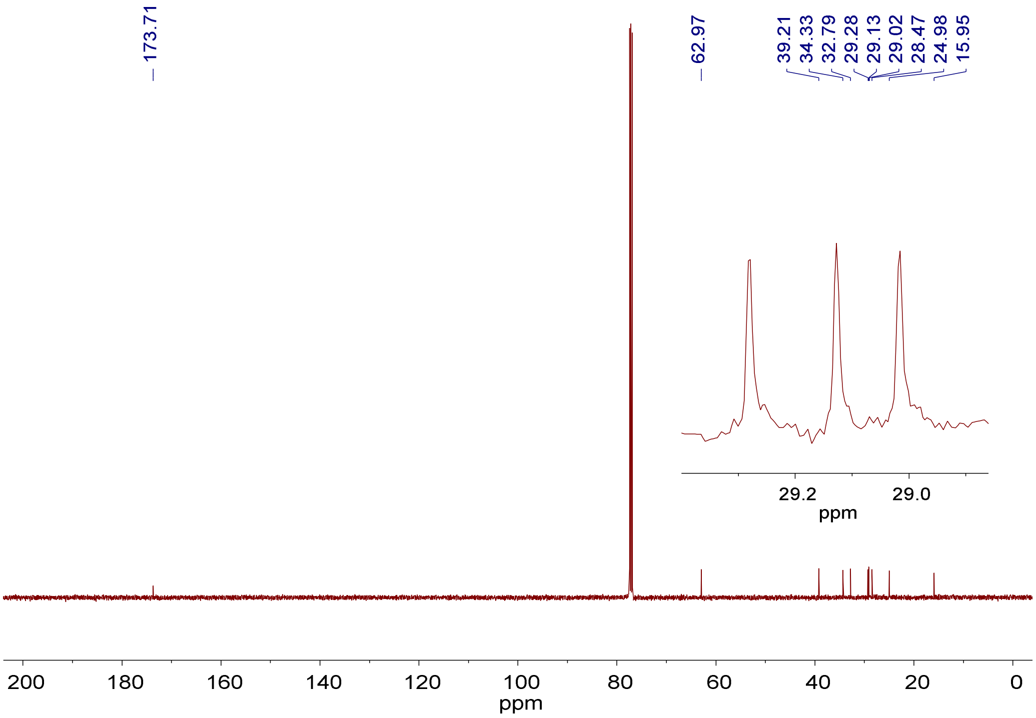

Figure S13. $^{13}C\{^1H\}$ NMR spectrum of **11-SMe** in $CDCl_3$.

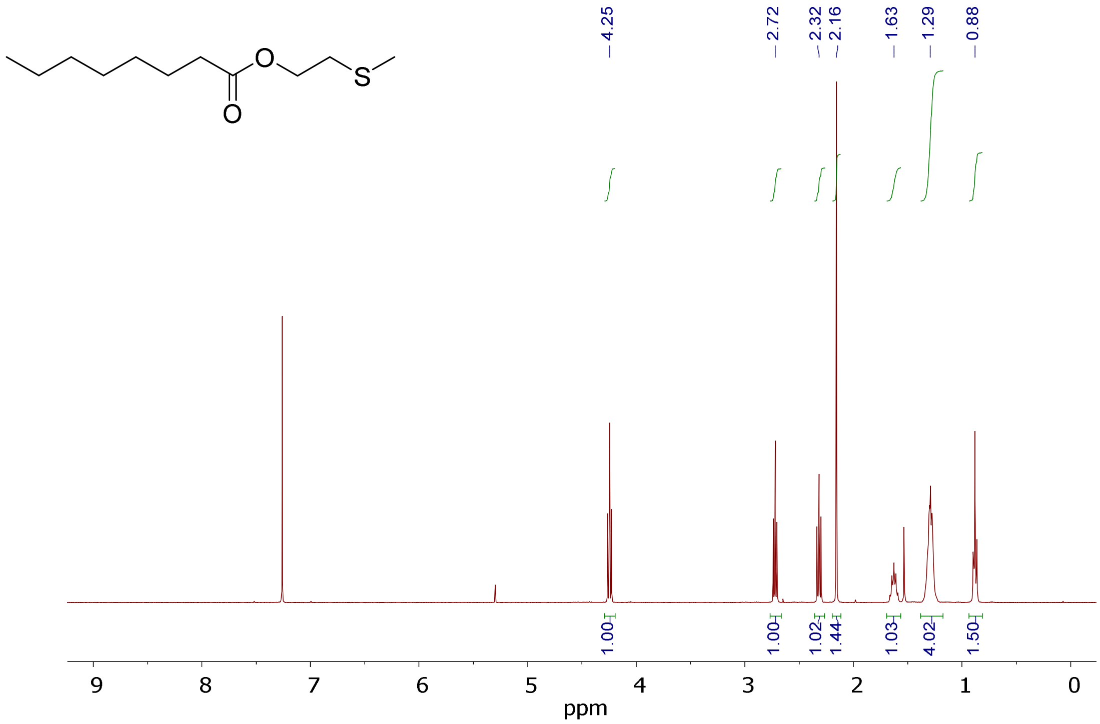

Figure S14. ^{1}H NMR spectrum of **3** in $CDCl_3$.

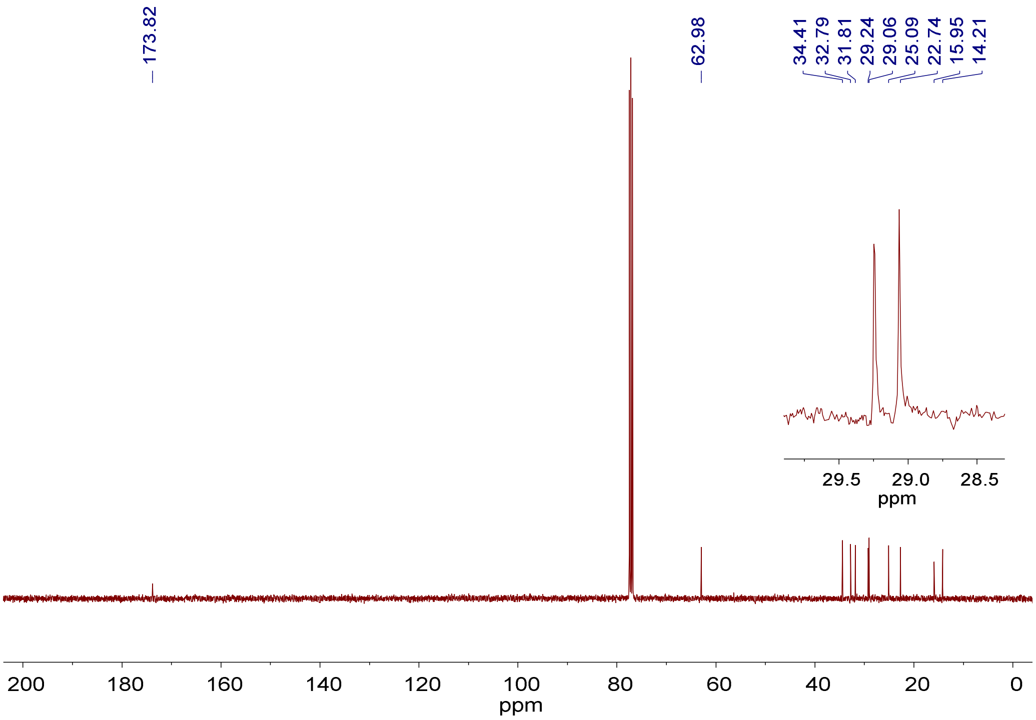

Figure S15. $^{13}C\{^{1}H\}$ NMR spectrum of **3** in $CDCl_3$.

6. References

1. L. Venkataraman, J. E. Klare, I. W. Tam, C. Nuckolls, M. S. Hybertsen and M. L. Steigerwald, *Nano Lett.*, 2006, **6**, 458-462.
2. M. M. Bader, *Phosphorus, Sulfur Silicon Relat. Elem.*, 1996, **116**, 77-92.
3. M. Kirihara, Y. Asai, S. Ogawa, T. Noguchi, A. Hatano and Y. Hirai, *Synthesis*, 2007, **2007**, 3286-3289.
4. V. Theodorou, K. Skobridis, A. G. Tzakos and V. Ragoussis, *Tetrahedron Lett.*, 2007, **48**, 8230-8233.